Microbial Biotechnology (2008) **1**(5), 382–394 doi:10.1111/j.1751-7915.2008.00033.x

Constructing and testing the thermodynamic limits of synthetic NAD(P)H:H_2 pathways

Andrea Veit, M. Kalim Akhtar, Taeko Mizutani and Patrik R. Jones*
Fujirebio Inc., Frontier Research Department, 51 Komiya-cho, Hachioji-shi, Tokyo 192-0031, Japan.

Summary

NAD(P)H:H_2 pathways are theoretically predicted to reach equilibrium at very low partial headspace H_2 pressure. An evaluation of the directionality of such near-equilibrium pathways *in vivo*, using a defined experimental system, is therefore important in order to determine its potential for application. Many anaerobic microorganisms have evolved NAD(P)H:H_2 pathways; however, they are either not genetically tractable, and/or contain multiple H_2 synthesis/consumption pathways linked with other more thermodynamically favourable substrates, such as pyruvate. We therefore constructed a synthetic ferredoxin-dependent NAD(P)H:H_2 pathway model system in *Escherichia coli* BL21(DE3) and experimentally evaluated the thermodynamic limitations of nucleotide pyridine-dependent H_2 synthesis under closed batch conditions. NADPH-dependent H_2 accumulation was observed with a maximum partial H_2 pressure equivalent to a biochemically effective intracellular NADPH/NADP$^+$ ratio of 13:1. The molar yield of the NADPH:H_2 pathway was restricted by thermodynamic limitations as it was strongly dependent on the headspace : liquid ratio of the culture vessels. When the substrate specificity was extended to NADH, only the reverse pathway directionality, H_2 consumption, was observed above a partial H_2 pressure of 40 Pa. Substitution of NADH with NADPH or other intermediates, as the main electron acceptor/donor of glucose catabolism and precursor of H_2, is more likely to be applicable for H_2 production.

Introduction

Molecular hydrogen is a promising energy carrier for both mobile and stationary applications in the future (Cho, 2004). Many bacteria and archaebacteria, with large variation in metabolic pathway diversity, are capable of producing and consuming H_2. In sugar-fermenting species, the most common glycolytic intermediate node for H_2 production is pyruvate, with either formate (for example *Enterobacter* spp.) (Wu, Wu *et al*., 1986; Sawers, 2005) or ferredoxin (formerly *Clostridium* spp.) (Thauer *et al*., 1971; Angenent *et al*., 2004) as intermediate electron acceptor/donors. Both reactions are thermodynamically favourable and will therefore proceed even at high partial pressure of H_2 with a maximum yield of 2 mol H_2 (mol glucose)$^{-1}$ (Angenent *et al*., 2004). The glyceraldehyde-3-phosphate (GAP) node is another important intermediate for which microorganisms have evolved both carbon-dependent (ethanol, lactate, butanol) and -independent (H_2) pathways to remove unwanted electrons generated through oxidation (Gottschalk, 1986). In most organisms, the nucleotide pyridine couple NADH/NAD$^+$ serves as the main electron acceptor/donor of GAP oxidation. Due to its central role in a large number of metabolically important reactions, the relative ratio of NADH/NAD$^+$ has important implications for overall metabolism and is maintained at measurable so-called 'steady-state' levels (Alexeeva *et al*., 2003). In theory, another 2 mol H_2 (mol glucose)$^{-1}$ could potentially be obtained from the GAP node by channelling all of the NADH generated in the GAPDH-dependent reaction towards H_2 formation by the following reaction (1):

$$NADH + H^+ \leftrightarrow NAD^+ + H_2 \quad (1)$$

NADH:H_2 pathways can potentially be catalysed either by multimeric NADH-dependent hydrogenases (Verhagen *et al*., 1999; Soboh *et al*., 2004; Vignais and Colbeau, 2004) or by the combined activities of three distinct proteins: NAD(P)H:ferredoxin oxidoreductase (NFOR), ferredoxin and hydrogenase (Jungermann *et al*., 1971; 1973; Thauer *et al*., 1971). Although extracts of several *Clostridium spp.* were earlier shown to catalyse NADH-dependent H_2 synthesis *in vitro* (Jungermann *et al*., 1971; 1973), not a single NFOR operating in a NADH:H_2 pathway has yet been identified at the gene sequence level.

There remains some question of whether NADH-dependent H_2 synthesis is metabolically relevant or not under conditions where H_2 is allowed to accumulate in the headspace (Jungermann *et al*., 1973). NADH-dependent

Received 16 October, 2007; revised 27 February, 2008; accepted 29 February, 2008. *For correspondence. E-mail js-patrik@fujirebio.co.jp; Tel. (+81) 426 45 4755; Fax (+81) 426 46 8325.

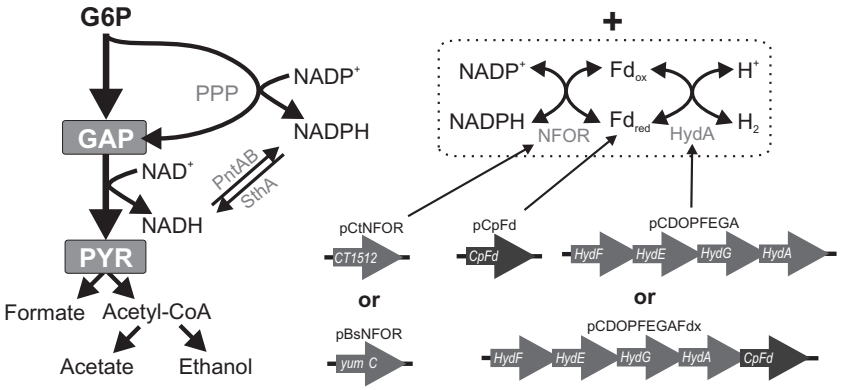

Fig. 1. Graphic illustration of anaerobic central carbon metabolism of importance for fermentative H_2 production in *E. coli* BL21(DE3). Pathways introduced in the present study are surrounded by a dotted rectangle. The plasmids employed to generate the pathways in the transformed host are indicated below. G6P, glucose-6-phosphate; GAP, glyceraldehyde-3-phosphate; PYR, pyruvate; PPP, pentose phosphate pathway; PntAB, membrane-bound NADPH:NADH transhydrogenase encoded by *pntAB*; SthA, soluble NADPH:NADH transhydrogenase encoded by *sthA*; NFOR, NAD(P)H:ferredoxin oxidoreductase; HydA, ferredoxin-dependent FeFe hydrogenase.

H_2 synthesis at reported cellular NADH/NAD^+ ratios is unlikely to be utilizable in a biotechnological process if the reaction reaches equilibrium at the very low partial pressure of H_2 (60 Pa) that has been theoretically predicted (Angenent *et al.*, 2004). Furthermore, it has been reported that the solubility of H_2 in microbial cultures can exceed the theoretical limit derived from Henry's Law by up to 80 times (Lamed *et al.*, 1988; Pauss *et al.*, 1990), potentially lowering the theoretical partial H_2 pressure limit for H_2 synthesis substantially further. In contrast, there are several convincing reports (Lamed *et al.*, 1988; Kumar *et al.*, 2001) suggesting that GAP-dependent H_2 synthesis indeed is operational in several microorganisms, even at partial H_2 pressure levels substantially above the limit suggested by Angenent and colleagues (2004). For example, based on fermentation balance analysis of mutant strains in which NADH-consuming reactions had been deleted, it was deduced that *Enterobacter aerogenes* most likely does catalyse NADH-dependent H_2 synthesis (Nakashimada *et al.*, 2002) even under closed batch conditions. Also, cultures of the extreme thermophile *Caldicellulosiruptor saccharolyticus* have been reported to generate H_2 yields above 3.0 mol H_2 (mol glucose)$^{-1}$ (de Vrije *et al.*, 2007) although H_2 productivity was unaffected by product accumulation until the partial H_2 pressure level reached above 5000 Pa (van Niel *et al.*, 2003). The main caveat with the preceding studies, however, is that the full complement of native H_2-metabolizing pathways, and their respective *in vivo* directionalities, remain unknown. Furthermore, as the pathways are not investigated in isolation, it is difficult to discriminate between them. Nevertheless, NADH-dependent H_2 synthesis reactions have been demonstrated in crude lysates of *E. aerogenes* (Nakashimada *et al.*, 2002) and it is difficult to believe that yields above 2.0 can be reached in any non-phototrophic species without oxidation of GAP. The question of whether NADH-dependent H_2 synthesis is thermodynamically limited or not therefore remains an open question until it can be verified using a defined experimental system. As utilization of GAP-dependent H_2 synthesis is critical in order to obtain reasonable H_2 yields, it is important to address this question to guide further research and development efforts towards enhancing microbial H_2 yield.

NADPH:H_2 pathways also exist in several microorganisms (Thauer *et al.*, 1971; Malki *et al.*, 1995; Silva *et al.*, 2000) and could theoretically be utilized to enhance H_2 production substantially, as demonstrated by Woodward and colleagues (2000) through *in vitro* reconstitution of pentose phosphate pathway-dependent H_2 production. However, the possibility of extending such a concept to *in vivo* production of H_2 is dependent on the outcome of a number of hitherto untested questions, including the directionality of NADPH:H_2 pathways. Several reports suggest that the pathway operates in the direction of $NADP^+$ reduction (Malki *et al.*, 1995; Steuber *et al.*, 1999), although this is yet to be convincingly demonstrated.

We engineered a synthetic NAD(P)H:H_2 pathway using *Escherichia coli* BL21(DE3) as a host. This strain differs substantially in H_2 metabolism from that of *E. coli* K-12 strains (Yoshida *et al.*, 2005; 2006; Maeda *et al.*, 2008), as it is effectively void of native H_2 metabolism (Akhtar and Jones, 2008a). The synthetic pathway consisted of a ferredoxin-dependent hydrogenase (King *et al.*, 2006; Akhtar and Jones, 2008b), a [4Fe4S] ferredoxin as intermediate electron acceptor/donor, and NFORs with specificity for either NADPH or NADH and NADPH (Fig. 1). This system was then used to experimentally determine to what degree NAD(P)H:H_2 pathways are thermodynamically limited *in vivo*, with ultimate consequences for pathway directionality.

Results

Construction of ferredoxin-dependent H_2 synthesis in E. coli *BL21(DE3)*

Prior to constructing the model system, we evaluated the H_2 metabolism of BL21(DE3) as a potential host. The accumulation and consumption of H_2 in closed cultures (headspace : liquid ratio of 2.2:1) of BL21(DE3) wild type,

in which the headspace contained either N_2 or 2% (v/v) H_2 (remainder N_2), was monitored over 52 h. BL21(DE3) pCDF-Duet (empty) accumulated H_2 (33 ± 6 Pa) to a level just above the limit of detection (~20 Pa) after 22 h, a level also observed using BL21(DE3) wild type (40 ± 6 Pa) even after 52 h of incubation. To cultures in which 2% (v/v) H_2 was added at the start of incubation, there was no change in the H_2 level even after 52 h. Together, this suggests that the native pyruvate formate lyase- and formate hydrogenlyase-dependent pathway (Sawers, 2005) effectively does not function in BL21(DE3) under the present experimental conditions, in contrast to *E. coli* K-12 strains (Yoshida *et al*., 2005; 2006; Maeda *et al*., 2008). Furthermore, as cultures of BL21(DE3) grown in MOPS minimal media glucose under anaerobic conditions do not consume added H_2, BL21(DE3) is therefore an ideal host for studying introduced or constructed H_2 metabolism, as it is effectively void of any form of H_2 metabolism.

As *E. coli* is not known to express a [4Fe4S] ferredoxin, the most likely native electron acceptor/donor partners of both *Clostridium acetobutylicum* HydA (Gorwa *et al*., 1996) and the thioredoxin reductase like NFORs (Seo and Sakurai, 2002; Seo *et al*., 2004), construction of NAD(P)H:H_2 pathways followed the two-step process of first introducing a recombinant [4Fe4S] ferredoxin, followed by the addition of NFORs. Successful synthesis of recombinant FeFe hydrogenase in *E. coli* BL21(DE3) was recently reported (Posewitz *et al*., 2004; King *et al*., 2006). Following on from this work, we constructed the plasmid pCDOPFEGA carrying a synthethic operon with genes encoding the three required FeFe hydrogenase maturation factors (Posewitz *et al*., 2004), and the FeFe hydrogenase HydA from *C. acetobutylicum* (Akhtar and Jones, 2008b). Strains carrying pCDOPFEGA and a separate plasmid allowing expression of either the gene encoding [4Fe4S] ferredoxin from *Clostridium pasteurianum* (CpFd, plasmid p4Fd) (Graves *et al*., 1985), or the gene encoding [2Fe2S] ferredoxin from *C. pasteurianum* (plasmid p2Fd) (Meyer *et al*., 1986), were prepared. Following overnight anaerobic expression, hydrogenase assays were initiated by the addition of dithionite to crude lysates. Reactions conducted with lysates expressing recombinant [4Fe4S] ferredoxin displayed three- to fourfold greater hydrogenase activity (9.5 ± 1.5 nmol H_2 min^{-1} mg^{-1}) compared with strains expressing [2Fe2S] ferredoxin (2.5 ± 1 nmol H_2 min^{-1} mg^{-1}) or no recombinant ferredoxin (2 ± 1 nmol H_2 min^{-1} mg^{-1}). Consequently, CpFd was chosen as a suitable candidate for further engineering and the gene encoding CpFd was added to pCDOPFEGA in order to generate the plasmid pCDOPFEGAFdx (Fig. 1).

Using small headspace cultures (headspace : liquid ratio of 0.6:1), the accumulation of H_2 in BL21(DE3) harbouring (i) pCDOPFEG (carrying only the hydrogenase maturation factors, negative control), (ii) pCDOPFEGA or (iii) pCDOPFEGAFdx was monitored for 22 h (Table 1). The addition of recombinant HydA to BL21(DE3) expressing the three hydrogenase maturation factors resulted in an increase in molar H_2 yield, an increase that was further enhanced in the dual presence of both HydA and CpFd (Table 1). This indicated that one or several native *E. coli* enzymes were capable of either directly or indirectly reducing both HydA and recombinant CpFd. We were interested in determining the unknown factor(s) responsible for H_2 synthesis in BL21(DE3) pCDOPFEGAFdx and therefore prepared deletion mutants of the two most likely candidates: *fpr* (annotated as the NADPH:flavodoxin/ferredoxin oxidoreductase Fpr) and *ydbK* (annotated as a putative pyruvate:flavodoxin/ferredoxin oxidoreductase, YdbK) (Blaschkowski *et al*., 1982), as well as the double mutant thereof. All three deletion strains accumulated H_2 with lower molar yield (Table 1), although Δ*fpr* deletion strains displayed poor growth under aerobic conditions (data not shown). BL21(DE3)Δ*ydbK* was therefore chosen as a host strain for further characterization of NFOR-dependent accumulation of H_2 *in vivo*, in order to limit H_2 metabolism by undefined pathways involving native enzyme(s). The fact that *E. coli* BL21(DE3) is capable of reducing the recombinant [4Fe4S] ferredoxin and HydA is surprising given that no [4Fe4S] ferredoxin, nor FeFe hydrogenase, has been reported in *E. coli*. The partial but incomplete reduction in CpFd- and HydA-dependent H_2 accumulation in response to the deletion of both *ydbK* and *fpr* suggests that other unknown proteins of *E. coli* with the capability of reducing CpFd and HydA must still remain. No obvious candidates exist in the genome, however (Serres *et al*., 2001).

Table 1. H_2 accumulation in BL21(DE3) in response to the expression of recombinant HydA and CpFd and to the deletion of *ydbK* and *fpr*.

Strains	H_2 yield [mmol H_2 (mol glucose)$^{-1}$]
BL21(DE3) pFEG	2.1 ± 0.3
BL21(DE3) pFEGA	3.5 ± 0.3
BL21(DE3) pFEGAFdx	5.2 ± 0.2
BL21(DE3)Δ*ydbK* pFEGAFdx	4.3 ± 0.1
BL21(DE3)Δ*fpr* pFEGAFdx	4.6 ± 0.3
BL21(DE3)Δ*ydbK*Δ*fpr* pFEGAFdx	4.2 ± 0.5

The molar yield of H_2 per mol of glucose was determined after 22 h of IPTG induction (0.05 mM) in MOPS minimal media using vessels with a headspace : liquid ratio of 0.6. Error bars indicate standard deviation ($n = 2$).

Construction of NAD(P)H:H_2 pathways in E. coli – *NADPH is a more suitable intermediate for H_2 production than NADH in* E. coli *BL21*

Recently, a NADPH:[4Fe4S] ferredoxin oxidoreductase from *Bacillus subtilis* (Seo *et al*., 2004) (BsNFOR), and a

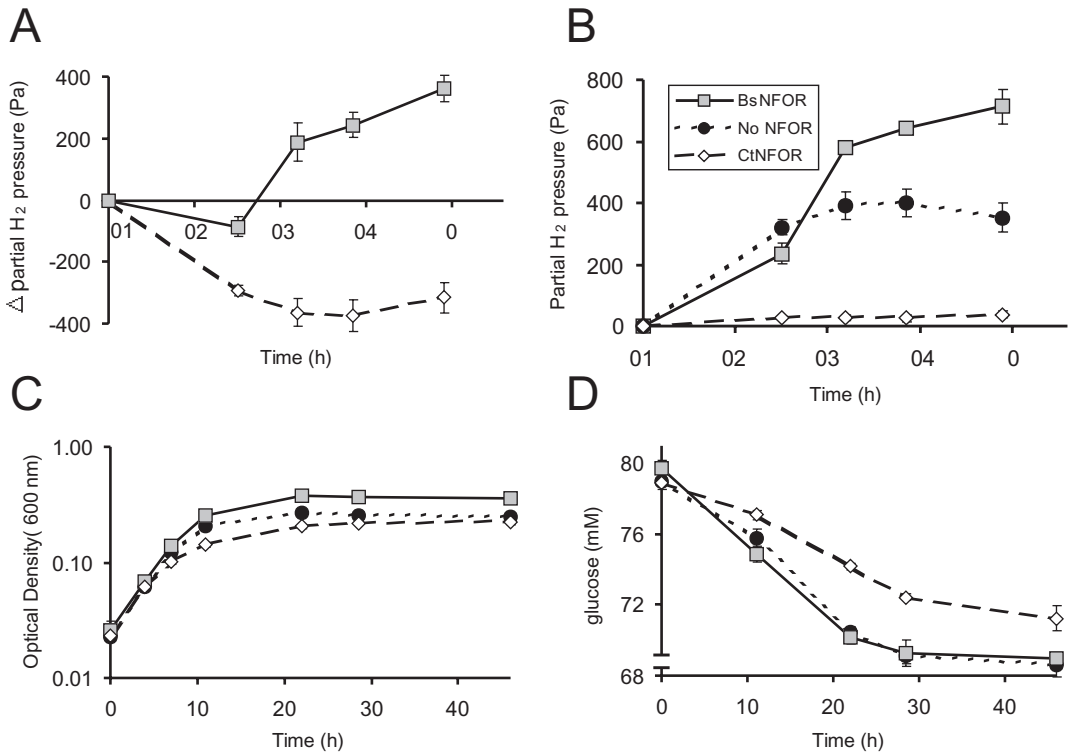

Fig. 2. A. The BsNFOR- (grey squares) and CtNFOR- (unfilled diamonds) dependent H_2 accumulation. The Δ partial H_2 pressure value is calculated by subtracting the partial H_2 pressure value of BL21(DE3)Δ*ydbK* pCDOPFEGA pCpFd pET-Duet from partial H_2 pressure values of cultures of BL21(DE3)Δ*ydbK* pCDOPFEGA pCpFd pCtNFOR or BL21(DE3)Δ*ydbK* pCDOPFEGA pCpFd pBsNFOR respectively.
B. Same as (A), except the actual partial H_2 pressure values for all three strains are shown [BL21(DE3)Δ*ydbK* pCDOPFEGA pCpFd pET-Duet, black circles; BL21(DE3)Δ*ydbK* pCDOPFEGA pCpFd pCtNFOR, empty diamonds; BL21(DE3)Δ*ydbK* pCDOPFEGA pCpFd pBsNFOR, grey squares].
C. Growth as determined by optical density (600 nm absorbance), for the same cultures as in (B).
D. Residual glucose (mM) in the media, for the same cultures as in (B).
Error bars indicate standard deviation ($n = 3$). All experiments were in vessels with a headspace : liquid ratio of 0.60.

NADPH and NADH:[4Fe–4S] ferredoxin oxidoreductase from *Chlorobium tepidum* (Seo and Sakurai, 2002) (CtNFOR) were described. The former enzyme, which has an unknown physiological role, is unlikely to be involved in H_2 metabolism as there are no reports that *B. subtilis* either consumes or produces H_2, while the latter enzyme is more likely to serve a role in photosynthesis similar to that of plant NADPH:[2Fe–2S] ferredoxin oxidoreductases (Carrillo and Ceccarelli, 2003). The heterologous expression, catalytic function and substrate specificity of recombinant BsNFOR and CtNFOR were confirmed by SDS-PAGE and activity assays (Appendix S1). No NADH-dependent reduction of methyl viologen (MV) was detected with crude extracts containing recombinant BsNFOR.

To construct NADPH and NADPH/NADH:H_2 pathways, the two NADH- and/or NADPH-dependent NFORs were coexpressed (in vessels with a headspace : liquid ratio of 0.6:1) along with CpFd and HydA. BsNFOR-dependent H_2 accumulation varied over time (Fig. 2). The maximum yield and partial H_2 pressure was achieved in strains coexpressing HydA, CpFd and BsNFOR, with partial H_2 pressure reaching a maximum of 770 Pa over 48 h in the small headspace vessels (Fig. 2). When expression of the NADPH-specific BsNFOR instead was substituted with the NADH- and NADPH-specific CtNFOR, H_2 accumulation was strongly reduced in comparison with strains in which no recombinant NFOR was expressed, and remained below 40 Pa throughout the whole cultivation period (Fig. 2). This suggests that the enhanced substrate specificity towards NADH displayed by CtNFOR results in a reversal in the directionality of the introduced pathway, i.e. consumption of H_2.

A comparison between strains with and without BsNFOR in small headspace vessels (headspace : liquid ratio of 0.6:1) showed that the introduced NADPH-dependent H_2 synthesis pathway only was effective after the cells had entered the stationary phase of growth (Fig. 2), a point at which the unknown native capability to reduce recombinant CpFd effectively stalled. In fact, strains expressing BsNFOR even displayed lower H_2 accumulation relative to strains expressing no NFOR at

the end of exponential phase, suggesting that NADPH was generated rather than consumed. After 28 h of cultivation, the yield of H_2 in cultures of BsNFOR-expressing strains, with and without subtraction of the yield obtained for cultures with strains where no recombinant NFOR was expressed, was 6.5 and 10.5 ($\pm$0.7) mmol H_2 (mol glucose)$^{-1}$ respectively. H_2 yields obtained from several independent experiments, although strongly dependent on the headspace : liquid ratio (as discussed below), varied between 10 and 40 mmol H_2 (mol glucose)$^{-1}$ at most. Additional overexpression of *E. coli* glucose 6-phosphate dehydrogenase (G6PDH; encoded by *zwf*) increased the total molar yield of H_2 to 96–192 mmol H_2 (mol glucose)$^{-1}$ (headspace : liquid ratio of 2.2); however, the glucose consumption of G6PDH-overexpressing cells was less than 50% compared with BL21(DE3) wild type. The molar yield of control strains, i.e. BL21(DE3) pET-Duet pCDOPFEGAFdx pCOLA*zwf*, under the same conditions was 26 mmol H_2 (mol glucose)$^{-1}$.

In order to verify the existence of functioning introduced pathways, cells were collected and lysed under anaerobic conditions, following 24–48 h of recombinant protein expression, and tested for NADH- and NADPH-dependent *in vitro* H_2 synthesis. The addition of cofactor regeneration systems was necessary in order to observe any product formation. In contrast to the *in vivo* results, extracts from hydrogenase- and ferredoxin-producing strains heterologously expressing CtNFOR displayed greater ability to catalyse NAD(P)H-dependent H_2 formation [110 $\pm$ 64 and 33 $\pm$ 13 nmol H_2 min^{-1} (mg protein)$^{-1}$ with NADPH and NADH respectively] than extracts prepared from cells expressing BsNFOR [70 $\pm$ 14 nmol H_2 min^{-1} (mg protein)$^{-1}$, NADPH only]. No H_2 was observed in the headspace with either cofactor, using crude extracts of negative controls, i.e. without expression of either recombinant NFOR or CpFd. Addition of 250 μM MV to *in vitro* reactions generally enhanced the rate of H_2 synthesis by a factor of 10–20. As increased H_2 evolution activities also were observed for purified *C. pasteurianum* HydA using a high concentration of MV relative to purified CpFdx (Fitzgerald *et al.*, 1980), an insufficient quantity of functional recombinant CpFdx is the most likely explanation for the large response to the addition of MV.

Testing the thermodynamic limitations of NAD(P)H-dependent H_2 synthesis

The partial hydrogen pressure at the equilibrium of reaction (1), in a closed space with a given molar cofactor ratio [NAD(P)H/NAD(P)$^+$], was estimated to be 35 and 142 Pa, for NADH and NADPH respectively, using Eqn A1 in Appendix S2. The estimation assumes that the cofactor ratio is fixed, that Henry's Law for the distribution of H_2 between the gaseous and liquid phase of only water applies, and uses previously reported values for nicotinamide cofactor content in *E. coli* under anaerobic conditions [0.75–0.88 for NADH/NAD$^+$, and 2.6 for NADPH/NADP$^+$ (Alexeeva *et al.*, 2003; Brumaghim *et al.*, 2003)] (Fig. 3A). The theoretical equilibrium of each H_2 pathway, depicted in Fig. 3A, is linearly related to the biochemically effective intracellular cofactor ratio, as the redox potentials of the two nucleotide couples are highly similar (Alberty, 2001). In order to experimentally verify that the NAD(P)H:H_2 pathway is thermodynamically limited in isolation, we affinity-purified recombinant HydA and CtNFOR under anaerobic conditions, and reconstituted the pathway *in vitro* with and without the addition of *Saccharomyces cerevisiae* G6PDH and glucose 6-phosphate (G6P) (Fig. 3B). As the addition of cofactor is finite the ratio of reduced to oxidized nicotinamide cofactor will vary during the reaction. The maximum possible partial H_2 pressure levels of the *in vitro* reaction without G6PDH were estimated to be 332 and 214 Pa for 5.5 and 12 ml headspace volume respectively, by determining the positive cofactor ratio at which the pressure derived from the ideal gas law (as given by Eqn A2 in Appendix S2) equals the pressure estimated at the equilibrium of reaction (1) given by Eqn A1. The experimentally determined partial H_2 pressure level reached approximately 30% and 45% [experimentally determined/theoretical predicted partial H_2 pressure (Pa)] for 5.5 and 12 ml headspace volume respectively, of the calculated theoretical maxima. The addition of G6PDH raised the maximum accumulated H_2 more than twofold. Yeast G6PDH was not able to reduce HydA directly or via any intermediate electron acceptor/donor as omission of BsNFOR abolished H_2 formation. The most plausible interpretation, of the effect of G6PDH on *in vitro* NADPH-dependent H_2 synthesis using purified components, is that the G6PDH maintained a low level of [NADP$^+$].

To test the effect of thermodynamic limitations on product accumulation *in vivo*, the headspace volume was varied while all other cultivation parameters were fixed. When the headspace volume of culture vessels was increased [headspace : liquid ratios of 5:1 and 31:1 (8 and 51 times larger than the small headspace cultures shown in Fig. 2 respectively)], the accumulation profile was significantly altered and the molar yield of H_2 increased (Fig. 4A). After 28 h, average BsNFOR-dependent H_2 yields (calculated by subtracting the yield observed with cultures using negative control strains, i.e. without expression of BsNFOR) were 4.9 ($\pm$0.7), 16.5 ($\pm$0.6) and 36.4 ($\pm$0.5) mmol H_2 (mol glucose)$^{-1}$ for cultures with a headspace : liquid ratio of 0.6:1, 5:1 and 31:1 respectively (Fig. 4C). The change in headspace affected both BsNFOR-independent and BsNFOR-dependent H_2 accumulation, as the molar yield of BsNFOR-independent H_2 accumulation over 28 h [7.0, 20.0 and 31.7 mmol H_2 (mol

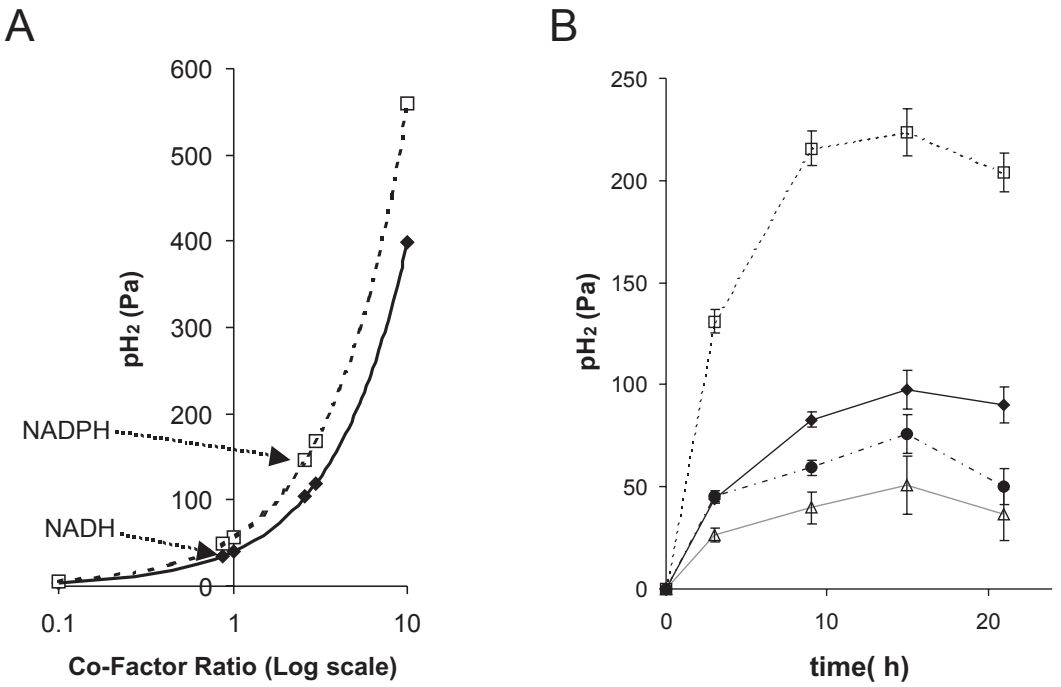

Fig. 3. A. The theoretical equilibrium point for a NADPH:H_2 (dashed line) and NADH:H_2 (solid line) pathway estimated using Eqn A2 in Appendix S2 assuming that the NAD(P)H/NAD(P)$^+$ ratio (cofactor ratio) is fixed. The equilibrium points calculated using cofactor ratios reported for *E. coli* cultured under anaerobic conditions (Alexeeva *et al*., 2003; Brumaghim *et al*., 2003) are highlighted with arrows.
B. *In vitro* reconstitution of NADPH-dependent H_2 synthesis using affinity-purified CtNFOR and HydA in closed N_2-sparged serum vessels. Standard reaction (filled diamonds) starts with 2.5 mM NADPH and uses serum vessels with a headspace of 5.5 ml. Variations: filled circles, 1.25 mM NADPH and 5.5 ml headspace; unfilled triangles, 2.5 mM NADPH and 12 ml headspace; unfilled squares, same as standard reaction except for addition of 4.5 U ml^{-1} G6PDH and 0.5 mM G6P. H_2 accumulation was also observed when NADPH was exchanged with NADH (standard reaction conditions: 42.3 $\pm$ 18.3 Pa H_2 at the 15 h sampling point). Error bars indicate standard deviation ($n = 3$).

glucose)$^{-1}$ in cultures with a headspace : liquid ratio of 0.6:1, 5:1 and 31:1 respectively] also was greater in the large headspace vessels. The only other parameter that is expected to change in response to variation in headspace volume is the partial pressure of CO_2. However, the addition of 2% (v/v) CO_2, a concentration we typically observed only after >24 h of growth in small headspace vessels, to large headspace vessel cultures at the start of induction did not affect H_2 accumulation or growth (data not shown).

To obtain an approximation of the *in vivo* equilibrium point for reaction (1) that was not influenced by growth stage-related changes to metabolism, H_2 was instead added at different levels to closed batch cultures (headspace : liquid ratio 2.2) after the cells had entered stationary phase. While cultures expressing BsNFOR accumulated hydrogen to partial H_2 pressure levels above 400 Pa, CtNFOR expressing cultures rapidly consumed H_2 down to a partial H_2 pressure level below 50 Pa (Fig. 4B). Rapid consumption of H_2 by CtNFOR-expressing cells supports the fact that the introduced pathway is functioning, although the directionality of the catalysed reaction is in the opposite direction of interest in cultures to which H_2 was added, but not in cultures to which H_2 was not added, as the latter cultures accumulated H_2 overall.

Based on the partial H_2 pressure levels that were obtained (as shown in Fig. 2B), we calculated the minimum intracellular NAD(P)H cofactor ratios using Eqn A1: 0.68 $\pm$ 0.13 (NADH/NAD$^+$, end of exponential phase), 0.91 $\pm$ 0.28 (NADH/NAD$^+$, late stationary phase), 4.3 $\pm$ 0.6 (NADPH/NADP$^+$, end of exponential phase), 13.1 $\pm$ 1.0 (NADPH/NADP$^+$, late stationary phase). We propose that these values are more likely to reflect biochemically effective intracellular cofactor ratios than those obtained by analysis using extracts, although accuracy will be improved further if all BsNFOR- and CtNFOR-independent H_2 synthesis can be completely removed and if an NFOR with strict specificity for only NADH can be obtained.

Discussion

In the present study we describe construction and verification of NAD(P)H:H_2 pathways and then use them to gain understanding regarding a fundamental issue which may pose a major stumbling block towards engineering for improved H_2 production, i.e. thermodynamic limita-

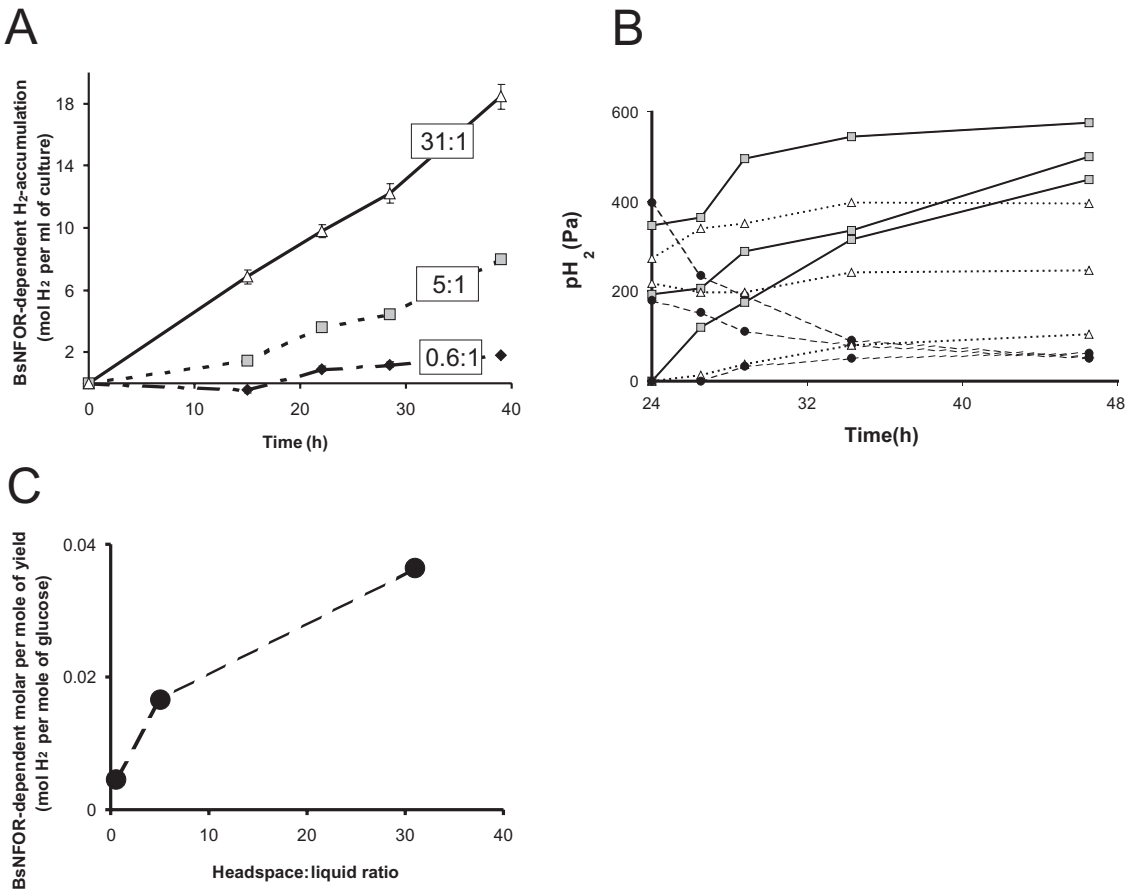

Fig. 4. A. The effect of headspace volume (filled diamonds, headspace : liquid ratio 0.6:1; grey squares, headspace : liquid ratio 5:1; open triangles, headspace : liquid ratio 31:1) on BsNFOR-dependent molar H_2 production. Molar differences in H_2 production were calculated by subtracting the average partial H_2 pressure value at each time point for cultures of strains harbouring pBsNFOR with average partial H_2 pressure values obtained from cultures of strains harbouring pET-Duet (i.e. no recombinant NFOR). All BL21(DE3)Δ*ydbK* strains also harboured pCDOPFEGA and pCpFd. The values are averages of differences between replicate culture pairs ($n = 3$). Error bars display standard deviation of differences between replicate culture pairs.
B. Consumption of H_2 by cultures of BL21(DE3)Δ*ydbK* harbouring pCDOPFEGAFdx and pBsNFOR (grey squares), pCtNFOR (unfilled triangles) or pET-Duet (filled circles). The headspace of independent replicate cultures was sparged with N_2 24 h after induction, followed by addition of three different levels of H_2 (0, ~125 Pa, ~300 Pa). The actual partial H_2 pressure of each individual culture measured directly following H_2 addition can be seen at t = 24, and the changes in partial H_2 pressure was thereafter monitored for an additional 24 h.
C. The relationship between the BsNFOR-dependent molar yield after 28 h of cultivation and the headspace to liquid ratio of the cultures shown in (A).
The values are averages of replicate cultures ($n = 3$).

tions. In addition, we also verify functional construction of NADPH-dependent H_2 synthesis, a pathway directionality which to date has not been demonstrated in any organism under growing conditions as far as we are aware. The turnover of NADP(H) in wild-type *E. coli* BL21 is expected to be lower than that of NAD(H) given that only ~5% of the total glycolytic flux will pass through the pentose phosphate pathway under anaerobic conditions (Fischer and Sauer, 2003). A proportion of NADH may also contribute towards NADPH under anaerobic conditions (Varma *et al.*, 1993) via the transhydrogenase PntAB, although the contribution by this route so far only has been quantified for *E. coli* K-12 strains under aerobic conditions (Sauer *et al.*, 2004). Consequently, the yield and rate of BsNFOR-dependent H_2 accumulation will ultimately be limited by a low turnover of NADP(H) under anaerobic conditions, and can therefore not be properly evaluated until that turnover has been enhanced. The use of defined controls in the present study, differing only in respect to whether a particular NFOR is present or absent, allowed the directionality and yield of the NFOR-dependent pathways to be evaluated, even though strains lacking BsNFOR also accumulated H_2.

The partial H_2 pressure level and H_2 yield of BL21(DE3)Δ*ydbK* pCDOPFEGA pCpFd pBsNFOR cultured in small headspace vessels (headspace : liquid ratio of 0.6) was at most twofold greater than the control strain that only differed by the absence of BsNFOR (Fig. 2).

Furthermore, the BsNFOR-dependent yield, at best (31:1 headspace : liquid ratio), did not exceed 40 mmol H_2 (mol glucose)$^{-1}$ (Fig. 4C). The relatively small response in H_2 accumulation to BsNFOR expression may be due to (i) a low turnover of NADP(H), (ii) thermodynamic limitations, affected by the headspace : liquid ratio and the intracellular NADPH/$NADP^+$ ratio and/or (iii) an insufficient catalytic capability by the introduced BsNFOR:CpFd:HydA pathway. The two- to fivefold response in H_2 yield from the BsNFOR-dependent pathway, imparted by coexpression of *E. coli* Zwf, suggests that poor catalytic capability is not limiting BsNFOR-dependent H_2 accumulation. This could also explain why trials with greater isopropyl-β-D-thiogalactopyranoside (IPTG) concentration did not enhance BsNFOR-dependent H_2 accumulation (data not shown). However, it does not distinguish between low turnover and thermodynamic limitations, as the presumed enhanced flux through the pentose phosphate pathway could potentially both increase NADP(H) turnover and the NADPH/$NADP^+$ ratio. The three- and sevenfold response in BsNFOR-dependent H_2 yield to increased headspace : liquid ratio (Fig. 4C), however, does suggest that the thermodynamic limitation constitutes the primary limitation that restricts BsNFOR-dependent H_2 accumulation in closed cultures with small headspace : liquid ratios. Nevertheless, as the response in H_2 yield to increased headspace : liquid ratio was lower when shifting from 5:1 to 31:1 than when shifting from 0.6:1 to 5:1 (Fig. 4C), we cannot fully exclude that also the other two limitations [(i) and/or (iii)] are affecting final H_2 yield.

While NADPH-dependent H_2 synthesis was functionally implemented with BsNFOR, only the apparent reverse pathway was observed with CtNFOR. When H_2 was absent in the headspace, oxidation of either NADPH, NADH and/or an unknown source of native reductant acted as a source of electrons to allow H_2 to accumulate just above the limit of detection (~30–40 Pa) (Fig. 2B). Once the partial H_2 pressure level reached the equilibrium point of both (NADPH:H_2 and NADH:H_2) pathways, no net flux occurred through the CtNFOR-dependent pathway in either direction. However, CpFd would still most likely be reduced by the unknown native source of reductant responsible for 'background' ferredoxin- and HydA-dependent H_2 production in the absence of any recombinant NFOR. The lack of increase in H_2 accumulation in such a case is most likely attributed to the oxidation of CpFd along with concomitant reduction of NAD^+ by CtNFOR, thus preventing any further delivery of electrons from CpFd to HydA. There is no doubt that the introduced CtNFOR-dependent pathway was operational, as crude lysates of CtNFOR-expressing cells catalysed both NADH- and NADPH-dependent H_2 synthesis with equal or greater rates than lysates of BsNFOR-expressing cells. Most convincingly, CtNFOR-expressing cells consumed added H_2 rapidly and to a lower final partial H_2 pressure value than strains expressing BsNFOR, while H_2 accumulation was observed in cultures to which no H_2 was added (Fig. 4B). Assuming that only one net directionality is possible by any given pathway, inhibition of CtNFOR by any unknown molecular effectors can thus be ruled out as a reason for near-zero H_2 accumulation. The strongly reduced equilibrium point, in CtNFOR- compared with BsNFOR-expressing strains, is therefore most likely a direct result of differences in the biochemically effective intracellular ratio of reduced to oxidized cofactor between the NAD(H) and NADP(H) couples. The differences in reported ratios obtained from the analysis of cellular extracts of *E. coli* [NADH/NAD^+ and NADPH/$NADP^+$ ratios: 0.88 versus 2.6 (Brumaghim *et al.*, 2003), 0.13 versus 1.3 (Andersen and von Meyenburg, 1977) respectively] support this conclusion. Pathway directionality for near-equilibrium reactions is therefore obviously more important than molar yield of precursor as the turnover of NADH per glucose most likely is >10-fold greater than that of NADPH in *E. coli*, as argued above.

In native organisms, there is only evidence of NADH-dependent H_2 synthesis (Jungermann *et al.*, 1971; Nakashimada *et al.*, 2002) and H_2-dependent $NADP^+$ reduction (Malki *et al.*, 1995; Steuber *et al.*, 1999). It has been suggested that NADPH and NADH has net cellular benefit and cost respectively (Varma *et al.*, 1993). The suggested directionalities for NADH:H_2 (H_2 synthesis) and NADPH:H_2 (H_2 consumption) pathways in native organisms would therefore theoretically make sense. However, there are issues with such a concept. First, physiologically unfavourable pathway directionalities would need to be restricted through regulatory mechanisms if external partial H_2 pressure levels do not favour the directionality of interest. This may explain why H_2-dependent NAD^+ reduction in *Clostridium* spp. was demonstrated to be restricted by sensitive feedback inhibition of the NFOR by NADH (Jungermann *et al.*, 1971; Thauer *et al.*, 1971), and why NADH-dependent hydrogenase activity of crude extracts of *Thermoanaerobacter tengcongensis* was markedly reduced in cells grown under closed, as opposed to open, headspace conditions (Soboh *et al.*, 2004). Second, how can GAP-dependent H_2 synthesis be physiologically relevant in native species, given that NADH-dependent H_2 synthesis is highly sensitive to end-product accumulation, and that the sensitivity most likely will be present regardless of whether a pathway is constructed or native? One possibility is that it is not metabolically relevant except in the special circumstance of very low partial H_2 pressure, as for example seen in syntrophic co-cultures shared with H_2-consuming methanogens (Lovley, 1985). Third, if H_2-dependent $NADP^+$ reduction is physiologically more favourable than the reverse directionality, as suggested by both theoretical (Varma *et al.*, 1993) and biochemical

analyses (Malki *et al.*, 1995; Steuber *et al.*, 1999), why then do we observe the reverse pathway directionality with the constructed pathway presented in the present study? This is most easily explained by the low partial H_2 pressure levels that were used in this study and a lack of evolved transcriptional regulation. Native NADPH-generating H_2 pathways may therefore only be metabolically relevant in environments with a high partial H_2 pressure level.

Theoretical prediction of pathway limitation is based on the assumption that 'fixed' cofactor ratios derived from post-extraction analysis can be used to predict pathway directionality for near-equilibrium reactions. Although it may be possible to measure a particular cofactor ratio in cellular extracts, is this exactly the ratio that influences >100 NAD(P)(H)-related reactions *in vivo*? Reported NADPH/NADP$^+$ cofactor ratios for *E. coli* vary greatly: 6.2 under aerobic conditions (Bautista *et al.*, 1979), 1.0 under aerobic conditions in exponential phase and 0.1 in stationary phase (Lee, Kim, Park and Lee *et al.*, 1996), 2.6 under anaerobic conditions and 0.11 under aerobic conditions (Brumaghim *et al.*, 2003), 0.5 under both anaerobic and aerobic conditions (Andersen and von Meyenburg, 1977), and 0.4 under aerobic conditions of both exponential and stationary phase (Walton and Stewart, 2004). A part of the variation is most likely due to the instability of NAD(P)H under conditions employed using existing extraction methods (Kimball and Rabinowitz, 2006; Pollak *et al.*, 2007; Rabinowitz and Kimball, 2007). In addition, the majority of intracellular NAD(P)H has been reported to be bound to enzymes (Patterson *et al.*, 2000) and it is not clear whether cofactors in the bound state could influence biochemical reactions differently from that of freely soluble cofactors (Pollak *et al.*, 2007). The ratio that determines the equilibrium point for NAD(P)H:H_2 pathways, the biochemically effective intracellular cofactor ratio, is therefore potentially influenced by at least two different parameters: (i) the total molar quantity of each cofactor form and (ii) the relative proportion of bound to free cofactor form. We determined the biochemically effective intracellular cofactor ratios using Eqn A1 and the experimentally determined partial H_2 pressure limits shown in Fig. 4. The differences between the ratios of the NADPH/NADP$^+$ and the NADH/NAD$^+$ couples were surprisingly large, a factor of 6 and 14 at the end of exponential and late stationary phase respectively. The estimated ratios for NADH/NAD$^+$ are within the range that is commonly reported 0.1–1.0, while the highest estimated ratio of NADPH/NADP$^+$ based on partial H_2 pressure levels is more than twofold above previously reported ratios (Andersen and von Meyenburg, 1977; Alexeeva *et al.*, 2003; Brumaghim *et al.*, 2003). The difference between partial H_2 pressure- and extraction-based ratios is most likely explained by the chemical lability of NAD(P)H, although it cannot be ruled out that the relative proportion of free to bound cofactor also could influence the equilibrium point.

The consistently large differences observed between the two cofactor couples are in line with conclusions derived from whole-cell thermodynamic *in silico* analysis, from which it was predicted that cofactor ratio estimates obtained from extraction-based analysis were close to the maximum (NADH/NAD$^+$) and minimum (NADPH/NADP$^+$) thermodynamically feasible ratios that would allow cellular metabolism and growth to proceed (Henry *et al.*, 2007). Interestingly, this suggests that there is potential for further increasing the NADPH/NADP$^+$ ratio, before reaching the point where whole-cell metabolism is predicted to be thermodynamically unfeasible. This is worth keeping in mind given that also NADPH-dependent H_2 synthesis is highly sensitive to end-product inhibition as shown in Fig. 4A, a degree of sensitivity that still may be too high for industrial application (van Groenestijn *et al.*, 2002), and that further studies are needed to explore the possibility of enhancing the biochemically effective intracellular NADPH/NADP$^+$ ratio.

In conclusion, we have constructed and verified two NAD(P)H:H_2 model pathways and demonstrated that both pathways are severely inhibited by end-product accumulation, although the equilibrium of the NADPH:H_2 pathway favoured H_2 accumulation to a greater extent than that of the NADH:H_2 pathway. Basing any future engineering on NAD(H) as a combined central carbon catabolite intermediate and H_2 precursor therefore appears impractical. However, some promise does exist for NADP(H), although low NADP(H) turnover is a major bottleneck that would need to be increased substantially to allow for any eventual application.

Experimental procedures

Chemicals and other reagents

All chemical reagents were obtained from SIGMA-Aldrich (Tokyo, Japan) except where stated. Restriction enzymes were from New England Biolabs (Hitchin, Hertfordshire, England). Genomic DNA for PCR amplification was either obtained directly from ATCC (*C. acetobutylicum* 824D-5, *C. tepidum* 49652D) or isolated from reference strains obtained from Deutsche Sammlung von Mikroorganismen und Zellkulturen GmbH (DSMZ) (*B. subtilis* DSM 402; *C. pasteurianum* DSM 525). Isolation of DNA was performed using the DNAeasy kit (Qiagen Sciences, MD, USA). SDS-PAGE was conducted using pre-cast 12% gels (TEFCO, Japan), gels were stained using SYPRO Orange (Invitrogen, Carlsbad, CA) and visualized using a Fujifilm FLA-3000 scanner according to manufacturer's instructions.

Bacterial strains, plasmids and growth conditions

The bacterial strains and plasmids used in this study are listed in Table 2 and all primers are listed in Table 3. Deletion

Table 2. Strains and plasmids used in the present study.

Strain or plasmid	Relevant characteristics	Source or reference
Strains		
MG1655	Wild type	CGSC
MG1655Δ*ydbK*::kan	MG1655 with *ydbK* deleted, kan^r	This study
MG1655Δ*fpr*::kan	MG1655 with *fpr* deleted, kan^r	This study
BL21(DE3)	*lon*$^-$, *ompT*$^-$	Novagen
BL21(DE3)Δ*fpr*	BL21(DE3) with *fpr* deleted	This study
BL21(DE3)Δ*ydbK*	BL21(DE3) with *ydbK* deleted	This study
BL21(DE3)Δ*ydbK*Δ*fpr*	BL21(DE3) with *ydbK* and *fpr* deleted	This study
Plasmids		
pCDF-Duet	Expression vector, spec^r	Novagen
pCOLA-Duet	Expression vector, kan^r	Novagen
pET-Duet	Expression vector, carb^r	Novagen
pET46-Ek/LIC	Expression vector, carb^r	Novagen
pCDOPFEG	pCDF-Duet with *C. acetobutylicum hydF* (CAC1651), *hydE* (CAC1631) and *hydG* (CAC1356) in MCS1 with MCS2 deleted	Akhtar and Jones (2008b)
pCDOPFEGA	pCDOPFEG- with addition of *C. acetobutylicum hydA* (U15277)	Akhtar and Jones (2008b)
pCDOPFEGAFdx	pCDOPFEGA with addition of gene encoding [4Fe4S] ferredoxin of *C. pasteurianum* (M11214)	This study
pBsNFOR	pET46-Ek/LIC with *yumC* of *B. subtilis* (CAB15201)	This study
pCtNFOR	pET46-Ek/LIC with gene encoding CtNFOR (CT1512) of *C. tepidum* (NP_662397)	This study
pCpFd	pCOLA-Duet with gene encoding [4Fe4S] ferredoxin of *C. pasteurianum* (M11214) in MCS1	This study
p4Fd	As above, except pET-Duet	This study
p2Fd	pET-Duet with gene encoding [2Fe2S] ferredoxin of *C. pasteurianum* (JH0804) in MCS1 with MCS2 deleted	This study
pCOLA*zwf*	pCOLA-Duet with *E. coli zwf* (b1852) in MCS1 with MCS2 deleted	M.O. Park and P.R. Jones (unpublished)
pKD13	kan^r, *oriR*γ	Datsenko and Wanner (2000)
pCP20	amp^r, yeast FLP recombinase	Datsenko and Wanner (2000)
pKD46	amp^r, *repA101*(ts), *araBP-gam-bet-exo*	Datsenko and Wanner (2000)

of the *ydbK* gene in *E. coli* MG1655 was performed according to the method of Datsenko and Wanner (2000). The FRT flanked kanamycin-resistance cassette of plasmid pKD13 was amplified by PCR using primers ydbK-for and ydbK-rev. After treatment with DpnI and purification, the deletion cassette was transformed to MG1655 WT carrying pKD46. Kanamycin-resistant clones were selected and the deletion was verified by PCR using primers K-ydbK-for and K-ydbK-rev. The resulting strain was designated MG1655Δ*ydbK*::kan and used as donor strain to generate BL21(DE3)Δ*ydbK* by P1 transduction (Miller, 1972) using BL21(DE3) (Novagen, Merck KGaA, Darmstadt, Germany) as recipient. After P1 transduction, the kanamycin-resistance gene was removed using the pCP20-encoded yeast recombinase (Datsenko and Wanner, 2000). Likewise the Δ*fpr* and Δ*ydbK*Δ*fpr* mutant of BL21(DE3) was obtained by P1 transduction using an MG1655Δ*fpr* strain (University of Wisconsin, USA) as the donor and BL21(DE3) and BL21(DE3)Δ*ydbK* as the respective recipient strains. The deletion of *fpr* was verified by PCR using primers K-fpr-for and K-fpr-rev.

Table 3. Oligonucleotides used in the present study.

Primer name	Sequence (5′ → 3′)
ydbK-for	CCCTCATTTGCGCAATGTAAGGGTGTCATATGATTACTATTGACGGGTGTAGGCTGGAGCTGCTTCG
ydbK-rev	GCAAATCAGCTGCAGCATCTTCCATAACTGTTCTGCCACTTCTGGATTCCGGGGATCCG
K-ydbK-for	GCGCAATGTAAGGGTGTCA
K-ydbK-rev	GTGCCAGGAAGTCATAGCG
K-fpr-for	GTCCATCCACTATCTGGATCG
K-fpr-rev	GATGATCAATAAGATGAGTGCG
BsNFOR-for	GACGACGACAAGATGCGTGAGGATACAAAGGTTTATG
BsNFOR-rev	GAGGAGAAGCCCGGTTTATTTATTTTCAAAAAGACTTGTTGAGTG
CtNFOR-for	GACGACGACAAGATGTTAGATATTCACAATCCAGCGACCGACC
CtNFOR-rev	GAGAGAAGCCCGGTTTACTCTGCCTTGTTCTCCGTCGCGTTGC
Cp4Fdx-for	ATCCATGGCATATAAAATCGCTGATTCATGTGTAAGC
Cp4Fdx-rev	TTTGTCGACTTATTCTTGTACTGGTGCTCCAACTGG
Cp2Fdx-for	TACCATGGTAAACCCAAAACACCACATATTCGTT TGTAC
Cp2Fdx-rev	TACCTAGGTTAAATTTGAAGTCTTTTAACAACTTCTC
FEGAFdx-for	ATAGGATCCGAATTTAAATAAAATGGCATATAAAATCGCTGATTCATG
FEGAFdx-rev	TACCT*AGGAGG*CCTCCTTTATTCTTGTACTGGTGCTCCAACTGGAC

Plasmids (Table 2), except for pCDOPFEGAFdx, were constructed using Accuprime PFX Polymerase (Invitrogen), primers (Table 3) and genomic DNA template as listed in Table 2 and vectors obtained from Novagen according to manufacturer's instructions. The insertion site for Ek/LIC vectors (pBsNFOR and pCtNFOR) is predetermined as described in manufacturer's instructions and all Ek/LIC-encoded gene products contained a vector-encoded N-terminal His-tag. All ferredoxin-encoding genes were cloned into MCS1 of pET-Duet or pCOLA-Duet using restriction sites NcoI and SalI (pCpFd and p4Fd) or AvrII (p2Fd), insertion sites that eliminate the native vector-encoded His-tag, using primers Cp4Fdx-for and Cp4Fdx-rev (pCpFd and p4Fd) and Cp2Fdx-for and Cp2Fdx-rev respectively. The plasmid pCDOPFEGAFdx was constructed by addition of the CpFd-encoding gene (M11214) at the 3' end of *hydA* in pCDOPFEGA using primers FEGAFdx-for and FEGAFdx-rev (Akhtar and Jones, 2008b). The identify of each plasmid gene construct was verified by sequencing and function was verified by SDS-PAGE and/or enzyme activity assay of crude lysates after test expression. The plasmids were used to transform strains by electroporation.

Cultivations were performed in 4–50 ml of MOPS minimal medium (Teknova, Hollister, CA) containing 1.5% glucose as carbon source, supplemented with kanamycin (50 μg ml^{-1}), carbenicillin (50 μg ml^{-1}) or spectinomycin (50 μg ml^{-1}), where appropriate. Pre-cultures were inoculated from a fresh Luria–Bertani (LB) plate and grown at 30°C to an OD_{600} of 0.1–0.5. Pre-cultures were then used to inoculate main cultures (same media with addition of 0.05 mM IPTG) at an approximate OD_{600} of 0.02. All cultures were grown at 30°C in serum vessels (35 or 125 mL) capped with butyl rubber septum and sparged with 99.9995% N_2 for >5 min following inoculation. Different levels of IPTG concentration were tested and 0.05 mM was found to be optimal for BsNFOR-dependent H_2 accumulation.

Leakage of H_2 from the serum bottles was assessed as follows. Four serum bottles (two containing 50 ml of MQ H_2O and the other two without any liquid) were capped with butyl rubber stoppers and exhaustively sparged (>5 min) with N_2 using one input needle and one outlet needle to retain atmospheric pressure. All bottles were then transferred into the anaerobic hood that had an atmosphere of ~5% H_2 and the butyl rubber stoppers removed. After >2 h of headspace gas equilibration, the same pierced butyl rubber stoppers were once again capped onto all four serum bottles. The H_2 content of all four bottles were measured by gas chromatography, and two of the serum bottles were again transferred into the anaerobic chamber (one with liquid, one without) while the other two were placed in an incubator (30°C, 175 r.p.m., 48 h). After 48 h, the H_2 content of all four bottles was once again determined. No detectable loss in H_2 was observed.

Heterologous gene expression and protein purification

All cell cultures expressing the FeFe hydrogenase were prepared exclusively under anaerobic conditions using buffers that were N_2-sparged prior to transfer into the anaerobic hood. Strains were grown at 30°C in terrific broth or LB media (Sambrook *et al*., 1989) containing 0.2–0.5 mM isopropyl β-D-1-thiogalactopyranoside for 18–36 h and then harvested by centrifugation (5000 *g*, 10 min, 4°C). Pelleted cells were re-suspended in 1/50th culture volume of lysis buffer [100 mM Tris·HCl (pH 7.5), 0.2 % Triton X-100, 2 mM dithiothreitol, 0.5–1.0 mg ml^{-1} chicken lysozyme (Wako Pure Chemical Industries, Osaka, Japan) and 50–200 U recombinant DNase I (Roche Diagnostics, Mannheim, Germany)] followed by freeze/thaw and incubation (10 min, 25°C). After the removal of cell debris by centrifugation (17 000 *g*, 10 min, 4°C), purification of HydA and BsNFOR was carried out using His SpinTrap columns (GE Healthcare Bio-Sciences AB, Uppsala, Sweden) according to manufacturer's instructions. Purified proteins were stored on ice until enzyme assays were performed.

In vitro *reconstitution*

Crude lysates (~1 μg of total protein) or His-tag purified protein preparations (0.024 U of hydrogenase, 0.6 U of NFOR), stored on ice inside an anaerobic hood, were added to 2 mL of N_2-sparged reaction mixtures [100 mM Tris.HCl (pH 7.5), 5% glycerol, 1 mM dithiothreitol, 1.25–2.5 mM NAD(P)H, 1 μM FAD, 250 μM MV]. Where indicated, 4.5 U ml^{-1} *S. cerevisiae* G6PDH and 0.5 mM G6P was added to regenerate NADPH, or 3 U ml^{-1} *Candida boidinii* formate dehydrogenase and 0.5 mM sodium formate was added to regenerate NADH. One U of enzyme activity corresponds to 1 μmol of product formed per min.

Enzyme assays

All assays were conducted under anaerobic conditions using quartz cuvettes fitted with open top screw cap (GL Sciences, Tokyo, Japan) and butyl rubber stopper (Voigt Global Distribution, Kansas City, USA). All reaction buffers and other additives were N_2-sparged prior to use. NAD(P)H-dependent reduction of MV was measured by following the reduction of MV at 600 nm (absorbance). Between 1 and 10 μg of crude protein or 0.5–1.0 μg of purified protein was added to N_2-sparged reaction mixture [50 mM Tris·HCl (pH 7.5), 10 μM flavine adenine dinucleotide, 0.5–1.0 mM NAD(P)H, 1 mM MV] to start the reaction. Dithionite- and hydrogenase-dependent synthesis of H_2 was measured by analysing the composition of the gaseous headspace of septum-closed serum bottles containing reaction mixtures (crude lysed cell extracts as described above, 0–0.5 mM MV, 10 mM Na_2SO_4) after incubation for up to 1–2 h at 30°C.

Analysis

Gaseous samples were analysed using a 6890N gas chromatograph (Agilent Technologies, Palo Alto, CA) fitted with a Carboxen™ (1010) PLOT capillary column (30 m × 0.32 mm) (Supelco, Bellefonte, USA). A 200 μl gas sample was withdrawn from the headspace of serum bottle cultures using a samplelock syringe (Hamilton, Reno, NV) and injected directly into the split/splitless inlet (ambient temperature, 5:1 split ratio). Samples were eluted isocratically (35°C, 4–5 min). The carrier gas was N_2 (17.6 ml min^{-1}) and a thermal conductivity detector (230°C, 2.0 ml min^{-1}) was used to detect samples. H_2 eluted at ~3.3 min and the partial headspace of H_2 (partial H_2 pressure) was quantified by comparisn with calibration curves prepared with 0.25% and 5%

standard H_2 gas samples (Kamimaru, Yokohama, Japan) and 100% H_2 (GL Sciences, Tokyo, Japan).

The glucose concentrations in the culture supernatants were determined using a D-glucose kit from Roche-Biopharm (Darmstadt, Germany) according to manufacturer's instructions.

Acknowledgments

We thank Myong-Ok Park for providing the functionally verified pCOLAzwf plasmid.

References

Akhtar, M.K., and Jones, P.R. (2008a) Deletion of *iscR* stimulates recombinant clostridial Fe–Fe hydrogenase activity and H_2-accumulation in *Escherichia coli* BL21(DE3). *Appl Microbiol Biotechnol* **78:** 853–862.

Akhtar, M.K., and Jones, P.R. (2008b) Engineering of a synthetic *hydF-hydE-hydG-hydA* operon for biohydrogen production. *Anal Biochem* **373:** 170–172.

Alberty, R.A. (2001) Standard apparent reduction potentials for biochemical half reactions as a function of pH and ionic strength. *Arch Biochem Biophys* **389:** 94–109.

Alexeeva, S., Hellingwerf, K.J., and Teixeira de Mattos, M.J. (2003) Requirement of ArcA for redox regulation in *Escherichia coli* under microaerobic but not anaerobic or aerobic conditions. *J Bacteriol* **185:** 204–209.

Andersen, K.B., and von Meyenburg, K. (1977) Charges of nicotinamide adenine nucleotides and adenylate energy charge as regulatory parameters of the metabolism in *Escherichia coli*. *J Biol Chem* **252:** 4151–4156.

Angenent, L.T., Karim, K., Al-Dahhan, M.H., Wrenn, B.A., and Domiguez-Espinosa, R. (2004) Production of bioenergy and biochemicals from industrial and agricultural wastewater. *Trends Biotechnol* **22:** 477–485.

Bautista, J., Satrustegui, J., and Machado, A. (1979) Evidence suggesting that the NADPH/NADP ratio modulates the splitting of the isocitrate flux between the glyoxylic and tricarboxylic acid cycles in *Escherichia coli*. *FEBS Lett* **105:** 333–336.

Blaschkowski, H.P., Neuer, G., Ludwig-Festl, M., and Knappe, J. (1982) Routes of flavodoxin and ferredoxin reduction in *Escherichia coli*. CoA-acylating pyruvate: flavodoxin and NADPH:flavodoxin oxidoreductases participating in the activation of pyruvate formate-lyase. *Eur J Biochem* **123:** 563–569.

Brumaghim, J.L., Li, Y., Henle, E., and Linn, S. (2003) Effects of hydrogen peroxide upon nicotinamide nucleotide metabolism in *Escherichia coli*. *J Biol Chem* **278:** 42495–42504.

Carrillo, N., and Ceccarelli, E.A. (2003) Open questions in ferredoxin-$NADP^+$ reductase catalytic mechanism. *Eur J Biochem* **270:** 1900–1915.

Cho, A. (2004) Fire and ICE: revving up for H_2. *Science* **305:** 964–965.

Datsenko, K.A., and Wanner, B.L. (2000) One-step inactivation of chromosomal genes in *Escherichia coli* K-12 using PCR products. *Proc Natl Acad Sci USA* **97:** 6640–6645.

Fischer, E., and Sauer, U. (2003) Metabolic flux profiling of *Escherichia coli* mutants in central carbon metabolism using GC-MS. *Eur J Biochem* **270:** 880–891.

Fitzgerald, M.P., Rogers, L.J., Rao, K.K., and Hall, D.O. (1980) Efficiency of ferredoxins and flavodoxins as mediators in systems for hydrogen evolution. *Biochem J* **192:** 665–672.

Gorwa, M.-F., Croux, C., and Soucaille, P. (1996) Molecular characterization and transcriptional analysis of the putative hydrogenase gene of *Clostridium acetobutylicum* ATCC 824. *J Bacteriol* **178:** 2668–2675.

Gottschalk, G. (1986) *Bacterial Metabolism*, 2nd edition. New York, NY, USA: Springer-Verlag.

Graves, M.C., Mullenbach, G.T., and Rabinowitz, J.C. (1985) Cloning and nucleotide sequence determination of the *Clostridium pasteurianum* ferredoxin gene. *Proc Natl Acad Sci USA* **82:** 1653–1657.

van Groenestijn, J.W., Hazewinkel, J.H.O., Nienoord, M., and Bussmann, P.J.T. (2002) Energy aspects of biological hydrogen production in high rate bioreactors operated in the thermophilic temperature range. *Int J Hydrogen Energy* **27:** 1141–1147.

Henry, C.S., Broadbelt, L.J., and Hatzimanikatis, V. (2007) Thermodynamics-based metabolic flux analysis. *Biophys J* **92:** 1792–1805.

Jungermann, K., Rupprecht, E., Ohrloff, C., Thauer, R., and Decker, K. (1971) Regulation of the reduced nicotinamide adenine dinucleotide-ferredoxin reductase system in *Clostridium kluyveri*. *J Biol Chem* **246:** 960–963.

Jungermann, K., Thauer, R.K., Leimenstoll, G., and Decker, K. (1973) Function of reduced pyridine nucleotide-ferredoxin oxidoreductases in saccharolytic *Clostridia*. *Biochim Biophys Acta* **305:** 268–280.

Kimball, E., and Rabinowitz, J.D. (2006) Identifying decomposition products in extracts of cellular metabolites. *Anal Biochem* **358:** 273–280.

King, P.W., Posewitz, M.C., Ghirardi, M.L., and Seibert, M. (2006) Functional studies of [FeFe] hydrogenase maturation in an *Escherichia coli* biosynthetic system. *J Bacteriol* **188:** 2163–2172.

Kumar, N., Ghosh, A., and Das, D. (2001) Redirection of biochemical pathways for the enhancement of H_2 production by *Enterobacter cloacae*. *Biotechnol Lett* **23:** 537–541.

Lamed, R.J., Lobos, J.H., and Su, T.M. (1988) Effects of stirring and hydrogen on fermentation products of *Clostridium thermocellum*. *Appl Environ Microbiol* **54:** 1216–1221.

Lee, Y., Kim, M.K., Park, Y.H., and Lee, S.Y. (1996) Regulatory effects of cellular nicotinamide nucleotides and enzyme activities on poly(3-hydroxybutyrate) synthesis in recombinant *Escherichia coli*. *Biotechnol Bioeng* **52:** 707–712.

Lovley, D.R. (1985) Minimum threshold for hydrogen metabolism in methanogenic bacteria. *Appl Environ Microbiol* **49:** 1530–1531.

Maeda, T., Sanchez-Torres, V., and Wood, T.K. (2008) Metabolic engineering to enhance bacterial hydrogen production. *Microb Biotechnol* **1:** 30–39.

Malki, S., Saimmaime, I., Luca, G., Rousset, M., Dermoun, Z., and Belaich, J.-P. (1995) Characterization of an operon encoding an NADP-reducing hydrogenase in *Desulfovibrio fructosovorans*. *J Bacteriol* **177:** 2628–2636.

Meyer, J., Bruschi, M.H., Bonicel, J.J., and Bovier-Lapierre, G.E. (1986) Amino acid sequence of [2Fe–2S] ferredoxin from *Clostridium pasteurianum*. *Biochemistry* **25:** 6054–6061.

Miller, J.H. (1972) *Experiments in Molecular Genetics*. Cold Spring Harbor, NY, USA: Cold Spring Harbor Laboratory Press.

Nakashimada, Y., Rachman, M.A., Kakizono, T., and Nishio, N. (2002) Hydrogen production of *Enterobacter aerogenes* altered by extracellular and intracellular redox states. *Int J Hydrogen Energy* **27:** 1399–1405.

van Niel, E.W., Claassen, P.A., and Stams, A.J. (2003) Substrate and product inhibition of hydrogen production by the extreme thermophile, *Caldicellulosiruptor saccharolyticus*. *Biotechnol Bioeng* **81:** 255–262.

Patterson, G.H., Knobel, S.M., Arkhammar, P., Thastrup, O., and Piston, D.W. (2000) Separation of the glucose-stimulated cytoplasmic and mitochondrial NAD(P)H responses in pancreatic islet beta cells. *Proc Natl Acad Sci USA* **97:** 5203–5207.

Pauss, A., Andre, G., Perrier, M., and Guiot, S.R. (1990) Liquid-to-gas mass transfer in anaerobic processes: inevitable transfer limitations of methane and hydrogen in the biomethanation process. *Appl Environ Microbiol* **56:** 1636–1644.

Pollak, N., Dolle, C., and Ziegler, M. (2007) The power to reduce: pyridine nucleotides – small molecules with a multitude of functions. *Biochem J* **402:** 205–218.

Posewitz, M.C., King, P.W., Smolinski, S.L., Zhang, L., Seibert, M., and Ghirardi, M.L. (2004) Discovery of two novel radical S-adenosylmethionine proteins required for the assembly of an active [Fe] hydrogenase. *J Biol Chem* **279:** 25711–25720.

Rabinowitz, J.D., and Kimball, E. (2007) Acidic acetonitrile for cellular metabolome extraction from *Escherichia coli*. *Anal Chem* **79:** 6167–6173.

Sambrook, J., Fritsch, E.F., and Maniatis, T. (1989) *Molecular Cloning: A Laboratory Manual*, 2nd edn. Cold Spring Harbor, NY, USA: Cold Spring Harbor Laboratory Press.

Sauer, U., Canonaco, F., Heri, S., Perrenoud, A., and Fischer, E. (2004) The soluble and membrane-bound transhydrogenases UdhA and PntAB have divergent functions in NADPH metabolism of *Escherichia coli*. *J Biol Chem* **279:** 6613–6619.

Sawers, R.G. (2005) Formate and its role in hydrogen production in *Escherichia coli*. *Biochem Soc Trans* **33:** 42–46.

Seo, D., and Sakurai, H. (2002) Purification and characterization of ferredoxin-NAD(P)$^+$ reductase from the green sulfur bacterium *Chlorobium tepidum*. *Biochim Biophys Acta* **1597:** 123–132.

Seo, D., Kamino, K., Inoue, K., and Sakurai, H. (2004) Purification and characterization of ferredoxin-NADP$^+$ reductase encoded by *Bacillus subtilis yumC*. *Arch Microbiol* **182:** 80–89.

Serres, M.H., Gopal, S., Nahum, L.A., Liang, P., Gaasterland, T., and Riley, M. (2001) A functional update of the *Escherichia coli* K-12 genome. *Genome Biol* **2:** RESEARCH0035.

Silva, P.J., Ban, E.C., Wassink, H., Haaker, H., de Castro, B., Robb, F.T., and Hagen, W.R. (2000) Enzymes of hydrogen metabolism in *Pyrococcus furiosus*. *Eur J Biochem* **267:** 6541–6551.

Soboh, B., Linder, D., and Hedderich, R. (2004) A multisubunit membrane-bound [NiFe] hydrogenase and an NADH-dependent Fe-only hydrogenase in the fermenting bacterium *Thermoanaerobacter tengcongensis*. *Microbiology* **150:** 2451–2463.

Steuber, J., Krebs, W., Bott, M., and Dimroth, P. (1999) A membrane-bound NAD(P)$^+$-reducing hydrogenase provides reduced pyridine nucleotides during citrate fermentation by *Klebsiella pneumoniae*. *J Bacteriol* **181:** 241–245.

Thauer, R.K., Rupprecht, E., Ohrloff, C., Jungermann, K., and Decker, K. (1971) Regulation of the reduced nicotinamide adenine dinucleotide phosphate-ferredoxin reductase system in *Clostridium kluyveri*. *J Biol Chem* **246:** 954–959.

Varma, A., Boesch, B.W., and Palsson, B.O. (1993) Stoichiometric interpretation of *Escherichia coli* glucose catabolism under various oxygenation rates. *Appl Environ Microbiol* **59:** 2465–2473.

Verhagen, M.F., O'Rourke, T., and Adams, M.W. (1999) The hyperthermophilic bacterium, *Thermotoga maritima*, contains an unusually complex iron-hydrogenase: amino acid sequence analyses versus biochemical characterization. *Biochim Biophys Acta* **1412:** 212–229.

Vignais, P.M., and Colbeau, A. (2004) Molecular biology of microbial hydrogenases. *Curr Issues Mol Biol* **6:** 159–188.

de Vrije, T., Mars, A.E., Budde, M.A., Lai, M.H., Dijkema, C., de Waard, P., and Claassen, P.A. (2007) Glycolytic pathway and hydrogen yield studies of the extreme thermophile *Caldicellulosiruptor saccharolyticus*. *Appl Microbiol Biotechnol* **74:** 1358–1367.

Walton, A.Z., and Stewart, J.D. (2004) Understanding and improving NADPH-dependent reactions by nongrowing *Escherichia coli* cells. *Biotechnol Prog* **20:** 403–411.

Woodward, J., Orr, M., Cordray, K., and Greenbaum, E. (2000) Enzymatic production of biohydrogen. *Nature* **405:** 1014–1015.

Wu, J.T., Wu, L.H., and Knight, J.A. (1986) Stability of NADPH: effect of various factors on the kinetics of degradation. *Clin Chem* **32:** 314–319.

Yoshida, A., Nishimura, T., Kawaguchi, H., Inui, M., and Yukawa, H. (2005) Enhanced hydrogen production from formic acid by formate hydrogen lyase-overexpressing *Escherichia coli* strains. *Appl Environ Microbiol* **71:** 6762–6768.

Yoshida, A., Nishimura, T., Kawaguchi, H., Inui, M., and Yukawa, H. (2006) Enhanced hydrogen production from glucose using *ldh*- and *frd*-inactivated *Escherichia coli* strains. *Appl Microbiol Biotechnol* **73:** 67–72.

Supporting information

Additional Supporting Information may be found in the online version of this article:

Appendix S1. Verification of the expression and activity of recombinant NFORs.

Appendix S2. Estimating the equilibrium point of reaction (1) and maximum partial H_2 pressure level for *in vitro* reaction employing finite starting substrate.

